Thin-Walled Structures 47 (2009) 912–918

Contents lists available at ScienceDirect

Thin-Walled Structures

journal homepage: www.elsevier.com/locate/tws

Simplification of the derivation of influence coefficients for symmetric frusta of shells of revolution

Alphose Zingoni *

Department of Civil Engineering, University of Cape Town, Rondebosch 7701, Cape Town, South Africa

ARTICLE INFO

Article history:
Received 12 September 2008
Accepted 22 February 2009
Available online 1 April 2009

Keywords:
Shell of revolution
Shell frustum
Shell analysis
Edge effects
Discontinuity effects
Influence coefficient
Spherical shell
Symmetric shell frustum

ABSTRACT

Shell-of-revolution frusta that possess symmetry in a plane perpendicular to the axis of revolution of the shell are often encountered as parts of bigger shell assemblies, and these frusta can have a wide variety of possible midsurface geometries such as spherical, ellipsoidal, toroidal, parabolic or hyperbolic. This paper presents a new technique for the simplification of the derivation of the influence coefficients for symmetric frusta of shells of revolution. The key strategy is the reduction of the number of unknowns of the problem by decomposing a system of arbitrary shell-edge actions into symmetric and anti-symmetric components conforming to the equatorial symmetry of the configuration.

1. Introduction

Shell-of-revolution frusta that possess symmetry in a plane perpendicular to the axis of revolution of the shell are often encountered as parts of bigger shell assemblies. We will refer to the plane of symmetry that is perpendicular to the axis of revolution of the shell as the "equatorial plane". Such symmetric shell frusta can have a variety of possible midsurface geometries such as spherical, ellipsoidal, toroidal, parabolic or hyperbolic. Some examples are illustrated in Fig. 1, where the axis of revolution of the shell is denoted by $R-R$ and the equatorial plane of symmetry is denoted by $E-E$. Here the shell frustum may represent the thickened part of an elevated liquid-containment shell in the zones around the supports (which are usually located at the equator for such tanks), or the edges of the frustum may simply be junctions of the frustum to another shell of different geometry (i.e. discontinuities in slope or radius of curvature of the shell meridian).

In analytical treatments of the axisymmetric bending of shells of revolution, a flexibility-type approach is often employed, where the membrane solution is taken as an approximate particular integral of the full bending-theory equations, while a system of axisymmetric bending moments and shearing forces applied upon the shell edges is taken as the homogeneous solution [1]. The latter will be referred to as "edge actions", and their effect upon the shell as the "edge effect". This approximation is known to be very accurate in the case of thin shells of radius-to-thickness ratio r/t greater than 30 (many shells in civil and mechanical engineering belong to this category), with errors being of the order of only t^2/r^2in comparison with unity [2,3]. This allows the stresses and deformations in the entire shell to be determined by superimposing the effects of the membrane solution with those of the edge actions.

In the flexibility analysis of thin axisymmetrically loaded shells of revolution, the edge actions are initially regarded as unknowns (or "redundants" in the terminology of the *force method* of structural analysis), and appropriate compatibility conditions must be imposed at the shell edges in order to allow the evaluation of these redundants [1]. In this process, we require the values of edge rotations and displacements associated with the surface loading (these are readily given by the membrane solution), as well as edge rotations and displacements associated with an arbitrary set of edge actions.

Fig. 2(a) shows an arbitrary set of axisymmetric edge actions applied upon the upper and lower edges of a symmetric shell-of-revolution frustum: $\{M_1, H_1\}$ at the upper edge, and $\{M_2, H_2\}$ at the lower edge. The actions $\{M_1, M_2\}$ are bending moments per unit length of the respective edge of the shell, while $\{H_1, H_2\}$ represent horizontal shearing forces per unit length of the shell edge (assuming the axis of revolution of the shell $R-R$ is vertical). Fig. 2(b) shows deformations arising at the shell edges as a result of the applied edge actions: $\{V_1, \delta_1\}$ at the upper edge, and $\{V_2, \delta_2\}$ at the lower edge. The deformations $\{V_1, V_2\}$ are rotations of the shell meridian (taken as positive when anticlockwise on the left of the axis of revolution of the shell), while $\{\delta_1, \delta_2\}$ are horizontal displacements of the shell (taken as positive when away from the axis of revolution of the shell).

* Tel.: +27 21 650 2601; fax: +27 21 689 7471.
E-mail address: alphose.zingoni@uct.ac.za

0263-8231/$ - see front matter © 2009 Elsevier Ltd. All rights reserved.
doi:10.1016/j.tws.2009.02.005

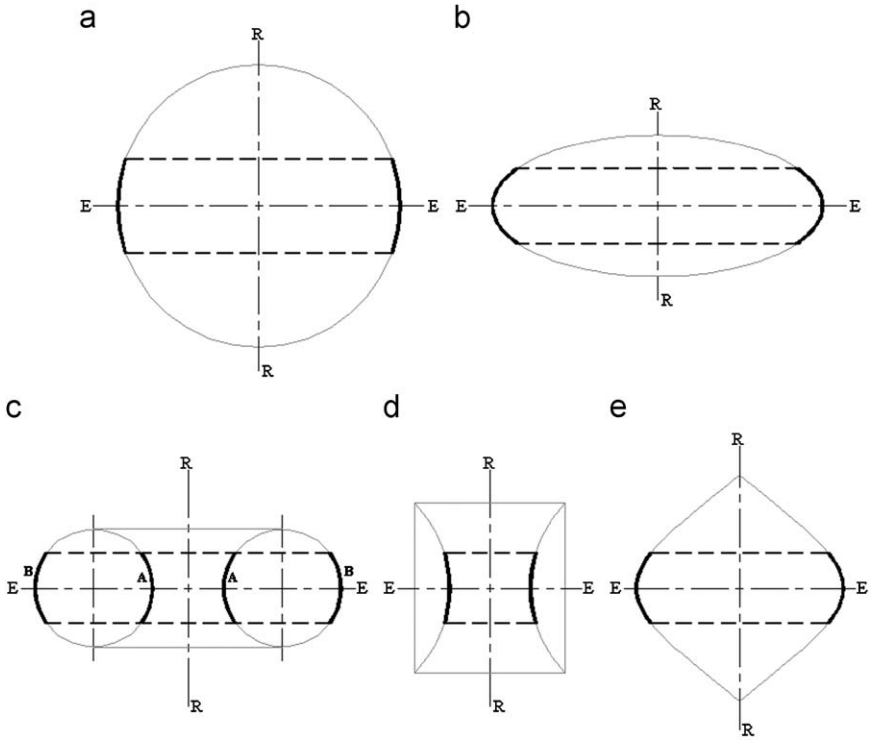

Fig. 1. Symmetric shell-of-revolution frusta: (a) spherical; (b) ellipsoidal; (c) toroidal; (d) hyperboloidal; (e) paraboloidal.

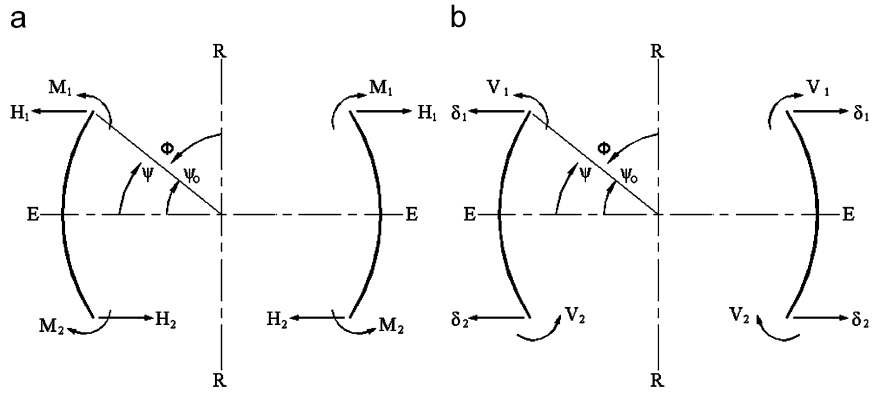

Fig. 2. Actions and deformations at the edges of a symmetric shell-of-revolution frustum (axis of revolution assumed to be vertical): (a) bending moments $\{M_1, M_2\}$ and horizontal shearing forces $\{H_1, H_2\}$; (b) rotations $\{V_1, V_2\}$ and horizontal displacements $\{\delta_1, \delta_2\}$.

We will adopt the coordinate ϕ to denote the meridional angle measured from the upward direction of the axis of revolution of the shell, to the normal to the shell midsurface at the point in question (Fig. 2). The alternative coordinate ψ denotes the meridional angle measured from the equatorial plane E–E to the normal to the shell midsurface at the point in question. From the diagrams, it is clear that the relationship $\psi = (\pi/2) - \phi$ holds. The parameter ψ_o is simply the value of ψ corresponding to the upper edge of the shell.

We may express the bending-related edge deformations in terms of the edge actions causing them in the following manner [1]:

$$\begin{bmatrix} V_1 \\ \delta_1 \\ V_2 \\ \delta_2 \end{bmatrix} = \begin{bmatrix} I_{11} & I_{12} & I_{13} & I_{14} \\ I_{21} & I_{22} & I_{23} & I_{24} \\ I_{31} & I_{32} & I_{33} & I_{34} \\ I_{41} & I_{42} & I_{43} & I_{44} \end{bmatrix} \begin{bmatrix} M_1 \\ H_1 \\ M_2 \\ H_2 \end{bmatrix} \tag{1}$$

The I_{ij} $(i = 1, \ldots, 4;\ j = 1, \ldots, 4)$ are the influence coefficients which, if known, enable the edge deformations caused by any system of edge actions $\{M_1, H_1, M_2, H_2\}$ to be fully evaluated. The determination of influence coefficients for various shells has received much attention in the past. For instance, Stern and Tsui [4] have obtained such coefficients for thin spherical-shell frusta on the basis of a practically exact solution for the axisymmetric bending of the spherical shell, whereas Zingoni and Pavlovic [5] have exploited an approximate but accurate solution for the axisymmetric bending of non-shallow spherical shells to derive influence coefficients for spherical-shell frusta. Both studies [4,5] also establish criteria that enable the bending effects at one edge of the spherical-shell frustum to be decoupled from those at the other edge, permitting a simplification of the shell analysis. However, the determination of influence coefficients for shells of revolution of more complex geometry remains a computationally challenging task, even if an exact mathematical solution for the shell-bending problem is known for the shell geometry in

question, since such solutions are generally cumbersome to implement in practical shell analyses. Here, we present a strategy that considerably simplifies the derivation of influence coefficients for symmetric shell-of-revolution frusta. Once such flexibility coefficients are known, they can easily be incorporated into computer programmes for the structural analysis of multi-shell assemblies.

Shell behaviour here is assumed to be linear elastic, which is generally valid for service conditions. Calculations based on the linear-elastic small-deformation theory of shells are very useful for gaining insight on the response of the shell under moderate loading conditions, and many existing shell structures have been successfully designed on the basis of this alone. Indeed modern design standards such as Eurocode 3 (for steel structures) allow room for such options [6,7]. Of course, nonlinear shell theories are required for studying the full spectrum of shell response, and for predicting shell behaviour near collapse [8]. Numerical modelling becomes indispensable for nonlinear problems. This is particularly so in the case of thin metal shells such as steel tanks and silos, where instability phenomena dominate shell behaviour, and the possibility of geometric imperfections has to be taken into account [6,7]. A comprehensive review of the literature on the buckling of thin shells has been given by Teng [9].

The analytical considerations of this paper are not material-specific, and equally apply to any isotropic shell, provided that the assumptions of shell behaviour being linear-elastic and shell geometry being perfect are reasonably accurate. Although valid for all non-shallow thin shells of revolution subjected to axisymmetric loading conditions, the approach is particularly useful for shells of double curvature (the type illustrated in Fig. 1).

2. Solution strategy for symmetric shell-of-revolution frusta

The strategy proposed here for the simplification of the solution procedure for shell influence coefficients is to decompose the system of arbitrary edge redundants $\{M_1, H_1, M_2, H_2\}$ into symmetric components $\{M_s, H_s\}$ and anti-symmetric components $\{M_a, H_a\}$, as depicted in Fig. 3. As we are concerned with only small elastic deformations of the shell, the principle of superposition is valid, and by reference to Fig. 3, we can write

$$M_1 = M_s + M_a; \quad H_1 = H_s + H_a \tag{2a}$$

$$M_2 = M_s - M_a; \quad H_2 = H_a - H_s \tag{2b}$$

where the symmetric and anti-symmetric components are given by

$$M_s = \frac{M_1 + M_2}{2}; \quad H_s = \frac{H_1 - H_2}{2} \tag{3a}$$

$$M_a = \frac{M_1 - M_2}{2}; \quad H_a = \frac{H_1 + H_2}{2} \tag{3b}$$

Finding the influence coefficients for the symmetric and anti-symmetric sub-systems of Fig. 3 involves only two unknowns for each sub-system, instead of the four unknowns of the original system. If we can obtain these (i.e. the sub-system influence coefficients), then the influence coefficients of the original system follow via linear combinations similar to the relations given by Eqs. (2a) and (2b).

Consider the deformations V_1 and δ_1 at the upper edge of the shell frustum (Fig. 2(b)). These may be written as linear combinations of symmetric and anti-symmetric components as follows:

$$V_1 = f_{11}M_s + f_{12}H_s + g_{11}M_a + g_{12}H_a \tag{4a}$$

$$\delta_1 = f_{21}M_s + f_{22}H_s + g_{21}M_a + g_{22}H_a \tag{4b}$$

Making use of the relations in Eqs. (3a) and (3b), we may express these deformations in the form

$$V_1 = f_{11}\left(\frac{M_1+M_2}{2}\right) + f_{12}\left(\frac{H_1-H_2}{2}\right) + g_{11}\left(\frac{M_1-M_2}{2}\right) + g_{12}\left(\frac{H_1+H_2}{2}\right) \tag{5a}$$

$$\delta_1 = f_{21}\left(\frac{M_1+M_2}{2}\right) + f_{22}\left(\frac{H_1-H_2}{2}\right) + g_{21}\left(\frac{M_1-M_2}{2}\right) + g_{22}\left(\frac{H_1+H_2}{2}\right) \tag{5b}$$

leading to the matrix form

$$\begin{bmatrix} V_1 \\ \delta_1 \end{bmatrix} = \begin{bmatrix} \left(\frac{f_{11}+g_{11}}{2}\right) & \left(\frac{f_{12}+g_{12}}{2}\right) & \left(\frac{f_{11}-g_{11}}{2}\right) & \left(\frac{-f_{12}+g_{12}}{2}\right) \\ \left(\frac{f_{21}+g_{21}}{2}\right) & \left(\frac{f_{22}+g_{22}}{2}\right) & \left(\frac{f_{21}-g_{21}}{2}\right) & \left(\frac{-f_{22}+g_{22}}{2}\right) \end{bmatrix} \times \begin{bmatrix} M_1 \\ H_1 \\ M_2 \\ H_2 \end{bmatrix} = \begin{bmatrix} a_{11} & a_{12} & b_{11} & b_{12} \\ a_{21} & a_{22} & b_{21} & b_{22} \end{bmatrix} \begin{bmatrix} M_1 \\ H_1 \\ M_2 \\ H_2 \end{bmatrix} \tag{6}$$

where the $\{a_{ij}, b_{ij};\ i = 1, 2;\ j = 1, 2\}$ are linear combinations of f_{ij} and g_{ij} $\{i = 1, 2;\ j = 1, 2\}$ as given on the first line.

From symmetry, and taking into account the sign convention in Fig. 2, the full flexibility relationships (upper and lower shell

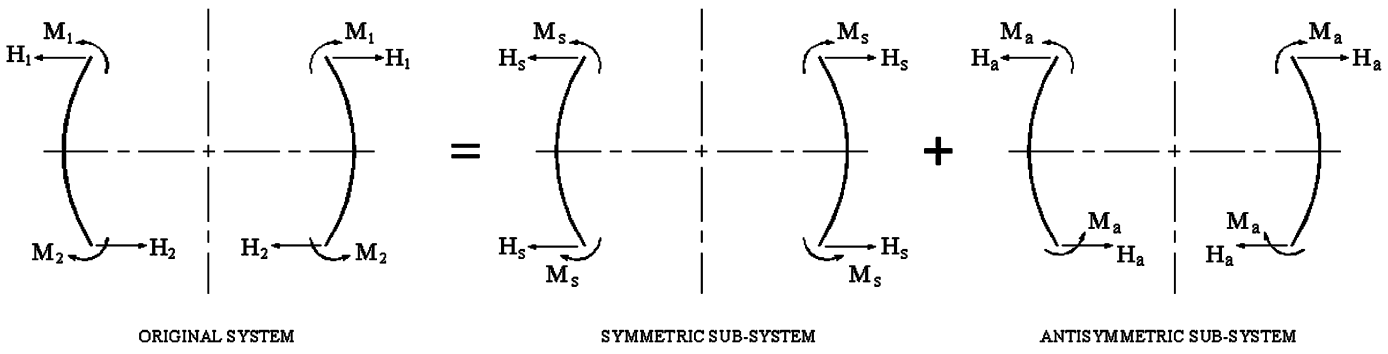

Fig. 3. Decomposition of the original system of edge actions $\{M_1, H_1, M_2, H_2\}$ into symmetric components $\{M_s, H_s\}$ and anti-symmetric components $\{M_a, H_a\}$.

edges taken together) are clearly

$$\begin{bmatrix} V_1 \\ \delta_1 \\ V_2 \\ \delta_2 \end{bmatrix} = \begin{bmatrix} a_{11} & a_{12} & b_{11} & b_{12} \\ a_{21} & a_{22} & b_{21} & b_{22} \\ b_{11} & b_{12} & -a_{11} & a_{12} \\ b_{21} & b_{22} & a_{21} & -a_{22} \end{bmatrix} \begin{bmatrix} M_1 \\ H_1 \\ M_2 \\ H_2 \end{bmatrix} \tag{7}$$

Thus all we need to evaluate are the eight parameters $\{a_{ij}, b_{ij}; i = 1, 2; j = 1, 2\}$.

3. Application to spherical-shell frusta

Symmetric spherical-shell frusta may be regarded as "non-shallow" if the angle ψ_o (Fig. 2) does not exceed 45°. Many spherical shell segments encountered in practical applications satisfy this condition. For such non-shallow spherical shells, the Geckeler approximation may be adopted as the theoretical basis for the estimation of edge effects in the shell. The Geckeler approximation is quite accurate in estimating the bending behaviour of thin spherical shells in regions where the angular coordinate ϕ is greater than 45° [10]. In those symmetric frusta where the total subtended angle $2\psi_o$ exceeds 90°, the two edges of the frustum would be sufficiently far apart anyway to permit a decoupled treatment of edge effects, for which the decomposition technique presented in this paper would not be necessary.

The Geckeler approximation applies more generally to all relatively steep-sided shells of revolution. It exploits the rapidly varying and highly damped character of edge bending effects, allowing the neglecting of lower-derivative terms of the Reissner–Meissner governing differential equations of bending of shells of revolution, in relation to higher-derivative terms [1,2]. The bending behaviour of the shell in the edge zone has a close analogy with the behaviour of a beam on an elastic foundation [11], and indeed some investigators have successfully developed solution procedures for specific shells of revolution on the basis of this analogy [12]. Guggenberger [13] has also pointed out an interesting analogy between shell edge bending and the deformation behaviour of a circular ring beam under eccentric axisymmetric loading. In combination with the membrane solution, Geckeler-type formulations provide a practical and effective theoretical basis for estimating the stresses in discontinuity zones of a variety of containment shell structures [14–17]. For thin spherical shells, the Geckeler approximation results in the equation

$$\frac{d^4 Q_\phi}{d\phi^4} + 4\lambda^4 Q_\phi = 0 \tag{8}$$

where Q_φ is the transverse shear force per unit length of the shell (as seen in the meridional section), ϕ is the meridional angle (measured as in Fig. 2) and λ is the shell-slenderness parameter, defined as follows:

$$\lambda^4 = 3(1-\nu^2)\frac{a^2}{t^2} \tag{9}$$

The parameters ν, a and t are the Poisson's ratio of the shell material, the shell radius and the shell thickness (assumed to be constant), respectively. Eq. (8) is similar to the governing equation for the axisymmetric bending of circular cylindrical shells. The general solution of the above differential equation may be written in terms of the angular coordinate ψ (refer to Fig. 2) as

$$\begin{aligned} Q_\phi = {} & C_1 \sin\lambda\psi \sinh\lambda\psi + C_2 \sin\lambda\psi \cosh\lambda\psi \\ & + C_3 \cos\lambda\psi \sinh\lambda\psi + C_4 \cos\lambda\psi \cosh\lambda\psi \end{aligned} \tag{10}$$

where $\{C_1, C_2, C_3, C_4\}$ are constants of integration. We may split the solution into components belonging to the symmetric and anti-symmetric deformation fields of the shell, as follows:

$$Q_s = C_2 \sin\lambda\psi \cosh\lambda\psi + C_3 \cos\lambda\psi \sinh\lambda\psi \tag{11a}$$

$$Q_a = C_1 \sin\lambda\psi \sinh\lambda\psi + C_4 \cos\lambda\psi \cosh\lambda\psi \tag{11b}$$

In the present approach, Eqs. (11a) and (11b) are considered separately. The objective is to obtain values of edge deformations $\{V_s, \delta_s\}$ and $\{V_a, \delta_a\}$ for the symmetric and anti-symmetric fields of deformations, respectively, on the basis of the solutions in Eqs. (11a) and (11b). Edge-related internal stress resultants $\{N_\phi^b, N_\theta^b\}$ and internal bending moments $\{M_\phi, M_\theta\}$ per unit length of the shell, in the meridional and hoop directions, respectively, as well as internal deformations $\{V^b, \delta^b\}$, are given by the following relations consistent with the Geckeler approximation [1]:

$$N_\phi^b = -Q_\phi \cot\phi = -Q_\phi \tan\psi \tag{12a}$$

$$N_\theta^b \approx -\frac{dQ_\phi}{d\phi} = +\frac{dQ_\phi}{d\psi} \tag{12b}$$

$$M_\phi \approx -\frac{a}{4\lambda^4}\frac{d^3 Q_\phi}{d\phi^3} = +\frac{a}{4\lambda^4}\frac{d^3 Q_\phi}{d\psi^3} \tag{13a}$$

$$M_\theta \approx \nu M_\phi \tag{13b}$$

$$V^b \approx \frac{1}{Et}\frac{d^2 Q_\phi}{d\phi^2} = \frac{1}{Et}\frac{d^2 Q_\phi}{d\psi^2} \tag{14a}$$

$$\delta^b \approx -\frac{a}{Et}(\sin\phi)\frac{dQ_\phi}{d\phi} = +\frac{a}{Et}(\cos\psi)\frac{dQ_\phi}{d\psi} \tag{14b}$$

The superscript b simply denotes that the effects are associated with the homogeneous bending problem (edge loading) rather than the membrane solution (surface loading). Note that $d\psi = -d\phi$ since $\psi = (\pi/2) - \phi$ (Fig. 2). Stress resultants follow the convention that tension is positive, while bending moments are considered positive if tending to reduce the curvature of the shell meridian (as in Fig. 2(a)).

Let us first consider the symmetric field of deformations. The shear force Q_ϕ assumes the value Q_s (Eq. (11a)). For the application of the edge action M_s at the upper edge of the shell (Fig. 3), the relevant boundary conditions are

$$(M_\phi)_{\psi=\psi_o} = M_s; \quad (N_\phi)_{\psi=\psi_o} = 0 \tag{15a,b}$$

Applying these boundary conditions to expressions (12a) and (13a) (with Q_s being given by Eq. (11a)) leads to the following solutions for the constants C_2 and C_3:

$$C_2 = \frac{f_2}{f_1(f_2+f_3) - f_4(f_2-f_3)}\left(\frac{2\lambda}{a}\right)M_s \tag{16a}$$

$$C_3 = \frac{-f_3}{f_1(f_2+f_3) - f_4(f_2-f_3)}\left(\frac{2\lambda}{a}\right)M_s \tag{16b}$$

where the parameters $\{f_1, f_2, f_3, f_4\}$ are defined as follows:

$$f_1 = \cos\lambda\psi_o \cosh\lambda\psi_o \tag{17a}$$

$$f_2 = \cos\lambda\psi_o \sinh\lambda\psi_o \tag{17b}$$

$$f_3 = \sin\lambda\psi_o \cosh\lambda\psi_o \tag{17c}$$

$$f_4 = \sin\lambda\psi_o \sinh\lambda\psi_o \tag{17d}$$

Similarly, for the application of the edge action H_s at the upper edge of the shell (Fig. 3), the relevant boundary conditions are

$$(M_\phi)_{\psi=\psi_o} = 0; \quad (N_\phi)_{\psi=\psi_o} = -H_s \sin\psi_o \tag{18a,b}$$

leading to the solutions

$$C_2 = \frac{f_1 + f_4}{f_1(f_2+f_3) - f_4(f_2-f_3)} \quad H_s \cos\psi_o \tag{19a}$$

$$C_3 = \frac{f_1 - f_4}{f_1(f_2+f_3) - f_4(f_2-f_3)} \quad H_s \cos\psi_o \tag{19b}$$

Evaluating at $\psi = \psi_o$ the deformations V^b and δ^b (Eqs. (14a) and (14b)) due to the application of M_s and those due to the application of H_s, using the respective values of the constants C_2 and C_3, and superimposing the results, we obtain the deformations at the upper edge

$$V_{s1} = \frac{2\lambda^2}{Et}\left[\frac{1}{f_1(f_2+f_3) - f_4(f_2-f_3)}\right] \times \left\{(f_2^2+f_3^2)\frac{2\lambda}{a}M_s + \{f_1(f_2-f_3) + f_4(f_2+f_3)\}H_s\cos\psi_o\right\} \tag{20a}$$

$$\delta_{s1} = \frac{\lambda a}{Et}(\cos\psi_o)\left[\frac{1}{f_1(f_2+f_3) - f_4(f_2-f_3)}\right]\{f_1(f_2-f_3) + f_4(f_2+f_3)\}\frac{2\lambda}{a}M_s + \{(f_1+f_4)^2 + (f_1-f_4)^2\}H_s\cos\psi_o\Big\} \tag{20b}$$

At the lower edge, we put $\psi = -\psi_o$ and obtain

$$V_{s2} = -\frac{2\lambda^2}{Et}(C_2 f_2 - C_3 f_3) = -V_{s1} \tag{21a}$$

$$\delta_{s2} = +\frac{\lambda a}{Et}(\cos\psi_o)\{C_2(f_1+f_4) + C_3(f_1-f_4)\} = \delta_{s1} \tag{21b}$$

as expected from symmetry.

We may therefore finally write the edge deformations for the symmetric field as follows:

$$\begin{bmatrix} V_s \\ \delta_s \end{bmatrix} = \frac{1}{f_1(f_2+f_3) - f_4(f_2-f_3)} \times \begin{bmatrix} (f_2^2+f_3^2)\frac{4\lambda^3}{Eat} & \{f_1(f_2-f_3) + f_4(f_2+f_3)\}\frac{2\lambda^2}{Et}\cos\psi_o \\ \{f_1(f_2-f_3) + f_4(f_2+f_3)\}\frac{2\lambda^2}{Et}\cos\psi_o & \{(f_1+f_4)^2 + (f_1-f_4)^2\}\frac{\lambda a}{Et}\cos^2\psi_o \end{bmatrix} \begin{bmatrix} M_s \\ \\ H_s \end{bmatrix} \tag{22}$$

The above is the symmetric part of Eqs. (4a) and (4b):

$$\begin{bmatrix} V_s \\ \delta_s \end{bmatrix} = \begin{bmatrix} f_{11} & f_{12} \\ f_{21} & f_{22} \end{bmatrix} \begin{bmatrix} M_s \\ H_s \end{bmatrix} \tag{23}$$

For the anti-symmetric field of deformations, the shear force Q_ϕ assumes the value Q_a (Eq. (11b)). We proceed in exactly the same steps as before, and end up with the following results for the edge deformations for the anti-symmetric field:

$$\begin{bmatrix} V_a \\ \delta_a \end{bmatrix} = \frac{1}{f_1(f_2-f_3) + f_4(f_2+f_3)} \times \begin{bmatrix} (f_1^2+f_4^2)\frac{4\lambda^3}{Eat} & \{f_1(f_2+f_3) - f_4(f_2-f_3)\}\frac{2\lambda^2}{Et}\cos\psi_o \\ \{f_1(f_2+f_3) - f_4(f_2-f_3)\}\frac{2\lambda^2}{Et}\cos\psi_o & \{(f_2+f_3)^2 + (f_2-f_3)^2\}\frac{\lambda a}{Et}\cos^2\psi_o \end{bmatrix} \begin{bmatrix} M_a \\ \\ H_a \end{bmatrix} \tag{24}$$

The above is the anti-symmetric part of Eqs. (4a) and (4b):

$$\begin{bmatrix} V_a \\ \delta_a \end{bmatrix} = \begin{bmatrix} g_{11} & g_{12} \\ g_{21} & g_{22} \end{bmatrix} \begin{bmatrix} M_a \\ H_a \end{bmatrix} \tag{25}$$

4. Final influence coefficients for the spherical shell

The full set of 16 influence coefficients for the bending of the symmetric spherical-shell frustum is given by Eq. (7), where the eight parameters $\{a_{ij},\ b_{ij};\ i=1,\ 2;\ j=1,\ 2\}$ are the linear combinations of the f_{ij} and g_{ij} $\{i=1,\ 2;\ j=1,\ 2\}$ as given in Eq. (6). The results for the f_{ij} are given by Eq. (22) read in conjunction with Eq. (23), while those for the g_{ij} are given by Eq. (24) read in conjunction with Eq. (25). Evaluating the a_{ij} and b_{ij} in accordance with the linear combinations of Eq. (6), we obtain the coefficients

$$\begin{aligned}
a_{11} &= \left\{\frac{f_2^2+f_3^2}{f_1(f_2+f_3) - f_4(f_2-f_3)} + \frac{f_1^2+f_4^2}{f_1(f_2-f_3) + f_4(f_2+f_3)}\right\} \times \frac{2\lambda^3}{Eat} = A_{11}\frac{2\lambda^3}{Eat} \\
a_{12} &= \left\{\frac{f_1(f_2-f_3) + f_4(f_2+f_3)}{f_1(f_2+f_3) - f_4(f_2-f_3)} + \frac{f_1(f_2+f_3) - f_4(f_2-f_3)}{f_1(f_2-f_3) + f_4(f_2+f_3)}\right\} \times \frac{\lambda^2}{Et}\cos\psi_o = A_{12}\frac{\lambda^2}{Et}\cos\psi_o \\
b_{11} &= \left\{\frac{f_2^2+f_3^2}{f_1(f_2+f_3) - f_4(f_2-f_3)} - \frac{f_1^2+f_4^2}{f_1(f_2-f_3) + f_4(f_2+f_3)}\right\} \times \frac{2\lambda^3}{Eat} = B_{11}\frac{2\lambda^3}{Eat} \\
b_{12} &= \left\{-\frac{f_1(f_2-f_3) + f_4(f_2+f_3)}{f_1(f_2+f_3) - f_4(f_2-f_3)} + \frac{f_1(f_2+f_3) - f_4(f_2-f_3)}{f_1(f_2-f_3) + f_4(f_2+f_3)}\right\} \times \frac{\lambda^2}{Et}\cos\psi_o = B_{12}\frac{\lambda^2}{Et}\cos\psi_o \\
a_{21} &= a_{12} \\
a_{22} &= \left\{\frac{(f_1+f_4)^2 + (f_1-f_4)^2}{f_1(f_2+f_3) - f_4(f_2-f_3)} + \frac{(f_2+f_3)^2 + (f_2-f_3)^2}{f_1(f_2-f_3) + f_4(f_2+f_3)}\right\} \times \frac{\lambda a}{2Et}\cos^2\psi_o = A_{22}\frac{\lambda a}{2Et}\cos^2\psi_o \\
b_{21} &= -b_{12} \\
b_{22} &= \left\{-\frac{(f_1+f_4)^2 + (f_1-f_4)^2}{f_1(f_2+f_3) - f_4(f_2-f_3)} + \frac{(f_2+f_3)^2 + (f_2-f_3)^2}{f_1(f_2-f_3) + f_4(f_2+f_3)}\right\} \times \frac{\lambda a}{2Et}\cos^2\psi_o = B_{22}\frac{\lambda a}{2Et}\cos^2\psi_o
\end{aligned} \tag{26a – h}$$

with the f_i $(i = 1, \ldots, 4)$ as previously defined (Eqs. (17a)–(17d)). The non-dimensional influence coefficients $\{A_{ij},\ B_{ij}\}$ (corresponding to the $\{a_{ij},\ b_{ij}\}$) are the terms in the braces of the above equations, and significantly, these are functions of only one parameter $\lambda\psi_o$.

Denoting by η the parameter $\lambda\psi_o$, we may plot the results for the non-dimensional influence coefficients $\{A_{11},\ A_{12},\ A_{22},\ B_{11},\ B_{12},\ B_{22}\}$ versus η. These plots are shown in Fig. 4, which may be used to read off the non-dimensional values for a shell frustum of any given radius a, shell thickness t or half-angle of opening ψ_o, and converted to actual influence coefficients via the multiplying factors in Eqs. (26a–h).

In these plots, notice that as the parameter η increases beyond $\eta = 1.2$, the coefficients A_{11} and A_{12} closely approach the limiting value of 2.0 while A_{22} approaches the limiting value of 4.0. The coefficients B_{11}, B_{12} and B_{22} tend towards zero but more slowly, only becoming rather insignificant when η exceeds 1.7. These limiting values for the non-dimensional influence coefficients are,

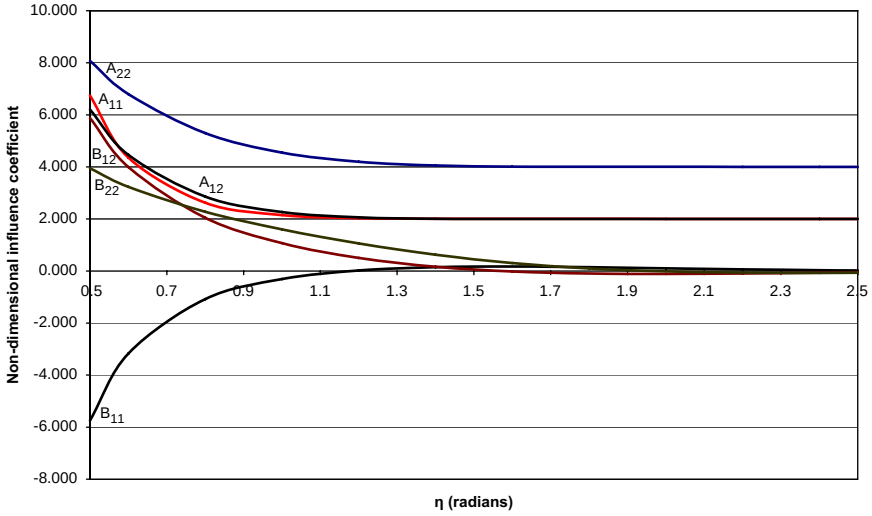

Fig. 4. Plots of non-dimensional influence coefficients $\{A_{ij}, B_{ij}\}$ for a symmetric spherical-shell frustum.

of course, the values corresponding to a decoupled analysis of edge effects, so in this sense the plots also provide pictorial estimates of the errors inherent in the common simplification of ignoring edge interaction in shell frusta.

5. Validation of results

The 16 influence coefficients for a general non-shallow spherical frustum (refer to Eq. (1)) have been previously derived via a computationally challenging conventional procedure that culminated in the following closed-form results for the influence coefficients [5]:

$$I_{11} = \frac{4\lambda^3}{Eat}\left[1 + \frac{2}{K}\{1 + 2\sin^2\beta + \sin 2\beta - e^{-2\beta}\}\right] \tag{27a}$$

$$I_{12} = \frac{2\lambda^2}{Et}(\sin\phi_1)\left[1 + \frac{2}{K}\{1 + 2\sin^2\beta - \cos 2\beta\}\right] \tag{27b}$$

$$I_{13} = -\frac{4\lambda^3}{Eat}\left[\frac{2}{K}\{e^{\beta}(\sin\beta + \cos\beta) + e^{-\beta}(\sin\beta - \cos\beta)\}\right] \tag{27c}$$

$$I_{14} = \frac{2\lambda^2}{Et}(\sin\phi_2)\left[\frac{4}{K}\sin\beta(e^{\beta} - e^{-\beta})\right] \tag{27d}$$

$$I_{21} = I_{12} \tag{27e}$$

$$I_{22} = \frac{2\lambda a}{Et}(\sin^2\phi_1)\left[1 + \frac{2}{K}\{1 + 2\sin^2\beta - \sin 2\beta - e^{-2\beta}\}\right] \tag{27f}$$

$$I_{23} = -\left(\frac{\sin\phi_1}{\sin\phi_2}\right)I_{14} \tag{27g}$$

$$I_{24} = \frac{2\lambda a}{Et}(\sin\phi_1)(\sin\phi_2)\left[\frac{2}{K}\{e^{\beta}(\sin\beta - \cos\beta) + e^{-\beta}(\sin\beta + \cos\beta)\}\right] \tag{27h}$$

$$I_{31} = -I_{13} \tag{27i}$$

$$I_{32} = -I_{23} = \left(\frac{\sin\phi_1}{\sin\phi_2}\right)I_{14} \tag{27j}$$

$$I_{33} = -I_{11} \tag{27k}$$

$$I_{34} = \left(\frac{\sin\phi_2}{\sin\phi_1}\right)I_{12} \tag{27l}$$

$$I_{41} = -I_{14} \tag{27m}$$

$$I_{42} = -I_{24} \tag{27n}$$

$$I_{43} = I_{34} = \left(\frac{\sin\phi_2}{\sin\phi_1}\right)I_{12} \tag{27o}$$

$$I_{44} = -\left(\frac{\sin^2\phi_2}{\sin^2\phi_1}\right)I_{22} \tag{27p}$$

where ϕ_1 and ϕ_2 are the values of the meridional-angle coordinate ϕ (refer to Fig. 2) corresponding to the upper and lower edges, respectively, of the shell frustum, and the parameters β and K are defined as follows:

$$\beta = \lambda(\phi_2 - \phi_1) \tag{28a}$$

$$K = e^{2\beta} + e^{-2\beta} - 2(1 + 2\sin^2\beta) \tag{28b}$$

Let us consider a numerical example, and compare the influence coefficients calculated on the basis of the present approach with those computed from Eqs. (27a)–(27p) above. The parameters chosen for the numerical example are

$$\frac{a}{t} = 100; \quad \nu = 0.15; \quad \psi_o = 10^{\circ} = 0.1745;$$
$$(\phi_2 - \phi_1) = 2\psi_o = 20^{\circ} = 0.3490$$

From Eq. (9), $\lambda = 13.0861$. Therefore $\eta = \lambda\psi_o = 2.2835$.

From Eqs. (17a)–(17d), $f_1 = -3.2409$; $f_2 = -3.1743$; $f_3 = +3.7500$; $f_4 = +3.6729$.

From Eqs. (28a) and (28b), $\beta = 4.5670$; $K = 9259.0920$.

Table 1 compares the influence coefficients a_{ij} and b_{ij} ($i = 1, 2$; $j = 1, 2$) as calculated using the present formulation for the symmetric spherical-shell frustum, versus their counterparts using the conventional approach of Ref. [5] (i.e. Eqs. (27a)–(27p) above). The results agree exactly (the tiny discrepancies are just rounding-off arithmetical errors), showing that the newly proposed formulation is completely valid and capable of giving the correct results.

Table 1
Validation of proposed formulation.

Results of present symmetric formulation	Results of conventional flexibility formulation [5]
$a_{11} = 2.0014(2\lambda^3/Eat)$	$I_{11} = 2.0014(2\lambda^3/Eat)$
$a_{12} = 2.0018(\lambda^2/Et)\cos\psi_o = a_{21}$	$I_{12} = 2.0016(\lambda^2/Et)\cos\psi_o = I_{21}$
$b_{11} = 0.0472(2\lambda^3/Eat)$	$I_{13} = 0.0472(2\lambda^3/Eat)$
$b_{12} = -0.0824(\lambda^2/Et)\cos\psi_o = -b_{21}$	$I_{14} = -0.0822(\lambda^2/Et)\cos\psi_o = -I_{23}$
$a_{22} = 4.0024(\lambda a/2Et)\cos^2\psi_o$	$I_{22} = 4.0024(\lambda a/2Et)\cos^2\psi_o$
$b_{22} = -0.0700(\lambda a/2Et)\cos^2\psi_o$	$I_{24} = -0.0704(\lambda a/2Et)\cos^2\psi_o$

6. Concluding remarks

In this article, a new approach has been presented for the computation of influence coefficients for frusta of thin shells of revolution that have symmetry about the equatorial plane. The key feature of the method is the decomposition of the deformation field into symmetric and anti-symmetric components, allowing the solution for constants of integration of the homogeneous shell-bending problem to be determined relatively easily. The influence coefficients of the original problem are obtained by linearly combining coefficients for the symmetric and anti-symmetric deformation fields. The procedure has been applied to the case of a spherical-shell frustum, and a numerical example used to validate the method.

The present method considerably simplifies the determination of influence coefficients for shells of revolution in question, and is particularly useful for tackling unusual shell geometries for which the governing equations of bending are difficult to solve. Even where the geometry of the shell midsurface is of well-known form (spherical, parabolic, ellipsoidal, toroidal, etc.), the thickness variation of the shell may be such that the governing shell-bending equations are complicated, and the homogeneous solution too cumbersome to apply. The proposed approach may be used to simplify the flexibility formulation of the problem.

In this study we have used the decomposition technique to generate closed-form analytical results for influence coefficients more conveniently. For shell-bending problems not amenable to exact mathematical solution, the present strategy can still be used in conjunction with numerical techniques (such as the differential quadrature method [18]) to simplify the solution of the relevant algebraic equations.

References

[1] Zingoni A. Shell structures in civil and mechanical engineering. London: Thomas Telford; 1997.
[2] Flügge W. Stresses in shells. Berlin: Springer; 1973.
[3] Seide P. Small elastic deformations of thin shells. Leiden: Noordhoff; 1975.
[4] Stern P, Tsui EYW. On the bending of spherical shells. J Eng Mech Div, ASCE 1966;92:53–66.
[5] Zingoni A, Pavlovic MN. On edge-disturbance interaction and decoupling errors in thin-walled nonshallow spherical-shell frusta. Thin-Walled Struct 1992;13:375–86.
[6] Rotter JM. Shell structures: the new European standard and current research needs. Thin-Walled Struct 1998;31(1-3):3–23.
[7] Rotter JM. Recent advances in the philosophy of the practical design of shell structures, implemented in Eurocode provisions. In: Zingoni A, editor. Recent developments in structural engineering, mechanics and computation. Rotterdam: Millpress; 2007. p. 26–31.
[8] Guggenberger W. Collapse design of large steel digester tanks. Thin-Walled Struct 1994;20(1-4):109–28.
[9] Teng JG. Buckling of thin shells: recent advances and trends. Appl Mech Rev 1996;49(4):263–74.
[10] Zingoni A, Pavlovic MN. Computation of bending disturbances in axisymmetrically loaded spherical shells: a study of the accuracy of Geckeler's approximation. Eng Comput 1990;7(2):125–43.
[11] Hetényi M. Beams on elastic foundation. Ann Arbor, USA: University of Michigan Press; 1946.
[12] Thambiratnam DP. A simple finite element analysis of hyperboloidal shell structures. Comput Struct 1993;48(2):249–54.
[13] Guggenberger W, Linder C. Analogy model for the axisymmetric elastic edge bending problem in shells of revolution based on Geckeler's approximation. In: Zingoni A, editor. Progress in structural engineering, mechanics and computation. London: Taylor & Francis; 2004. p. 269–74.
[14] Zingoni A. Stresses and deformations in egg-shaped sludge digesters: membrane effects. Eng Struct 2001;23(11):1365–72.
[15] Zingoni A. Stresses and deformations in egg-shaped sludge digesters: discontinuity effects. Eng Struct 2001;23(11):1373–82.
[16] Zingoni A. Parametric stress distribution in shell-of-revolution sludge digesters of parabolic ogival form. Thin-Walled Struct 2002;40(7,8):691–702.
[17] Zingoni A. Discontinuity effects at cone–cone axisymmetric shell junctions. Thin-Walled Struct 2002;40(10):877–91.
[18] Redekop D. Buckling analysis of an orthotropic thin shell of revolution using differential quadrature. Int J Press Vessel Pip 2005;82:618–24.